DOI: 10.48011/asba.v2i1.1664

Offline FMPC Applied to the 3SSC Boost Converter

Thalita B. S. Moreira * **Marcus V. S. Costa** *
F. G. Nogueira **

* *Electrical Engineering Graduate Program, Federal Rural University of the Semi-Arid Region, Mossoró, RN, Brazil (e-mail: marcus.costa@ufersa.edu.br, thalita_brenna@hotmail.com).*
** *Federal University of Ceará, Fortaleza, Brazil, (e-mail: fnogueira@ufc.br)*

Abstract: This article develops a novel application for fuzzy model predictive control (FMPC), applying this control law to a three state-switching cell (3SSC) boost converter. The converter is modeled using augmented state space equations through a polytopic approach, associated with fuzzy membership functions in order to reject disturbances caused by the change in the operating point. Furthermore, the FMPC combines Model Predictive Control (MPC), Takagi-Sugeno (T-S) and Parallel-Distributed Compensation (PDC) fuzzy methodologies. In addition, an offline approach for the FMPC is presented, whose gains are obtained via stability ellipsoids and stored in a lookup-table. The obtained results highlight the performance of the proposed method in comparison with the benchmark controller, through analysis of time responses, stability ellipsoids and performance index J_∞.

Keywords: Fuzzy Control, Model Predictive Control, 3SSC Boost Converter, Linear Matrix Inequalities, Stability Ellipsoid, Offline FMPC.

1. INTRODUCTION

The advances on methods and computation capacity of microprocessors allowed the development and application of powerful and sophisticated control strategies (Vazquez et al., 2016), among these strategies stand out the model predictive control (MPC) and the fuzzy control. These control techniques feature useful advantages and can be applied in several fields; recent applications can be seen in Sari et al. (2019), Fateh and Fateh (2020) and Bartsch et al. (2019).

According to Wang (2009), the MPC has been widely used in industrial and academic applications, due to its attractive features. The MPC consists of different control methods that share common aspects. Some examples of these strategies are the Generalized Predictive Control (GPC), the Robust Model Predictive Control (RMPC) and the Dynamic Matrix control (DMC). The main property of MPC is the prediction ability in a process model. Moreover, MPC strategies execute a control law that minimizes a certain cost function over a prediction horizon (Camacho and Bordons, 2007).

Among MPC's methods, the procedure developed by Kothare et al. (1996) highlights. This controller found many applications due to its capacity to guarantee the stability and performance, even when subject to system constraints, model uncertainties, multivariable process, disturbances and time delay. Evidences of the success of this approach can be found in Maccari Jr et al. (2019), Rego and Costa (2020), and Capron and Odloak (2013). Nonetheless, this control strategy presents difficulties in controlling complex nonlinear systems as confirmed in Khairy et al. (2010) and Yu-Geng et al. (2013).

Oppositely, fuzzy controllers are well suitable for dealing with nonlinear models. According to Kovacic and Bogdan (2006), this aspect explains the increase in applications using this approach. The Takagi-Sugeno (T-S) methodology offers a way to model systems using fuzzy theory, and is popular because of its proven feature as an universal approximator (Takagi and Sugeno, 1985). In this context, Lu (2018), Treesatayapun (2019) and Abbasi and Jalali (2020) illustrate promise results using fuzzy techniques.

Many researchers found a good solution to the disadvantages of MPC through the association of fuzzy control with MPC, as pointed by Espinosa et al. (1999). Recent developments for the Fuzzy Model Predictive Control (FMPC) can be explore in Wu et al. (2015), Méndez et al. (2016), Teng et al. (2017), and Wang et al. (2018).

Considering the FMPC positive background, this study proposes a novel application of the FMPC applied to the three-state switching cell (3SSC) boost converter. The power electronics field is an attractive application for advanced control techniques. According to Costa (2017), this interest is based on the need to use robust control methods to assure the stability of these systems, even in the presence of disturbance, change of the operating point, and constraints to the process.

Thus, this article proposes the following contributions: (1) a system model using the augmented state space equations associated with fuzzy membership functions and a polytopic structure; (2) applying the FMPC to the converter through the T-S and Parallel-Distributed Compensation (PDC) fuzzy methods, aiming at a stable system using state-feedback gains; (3) an offline formulation of the FMPC using the stability ellipsoids stored in a lookup-table; (4) a comparison between the FMPC and the classic Linear Quadratic Integral (LQI), described in Luong and Tsao (2014), under the same design conditions.

The results obtained in this study evidences the effectiveness of the proposed FMPC applied to output voltage control of the 3SSC Boost converter. The presented paper adopts the output time response considering the disturbances originated from the input voltage and load. Also, the lookup table is displayed using the impulsive response data of x_{set} provided by Costa (2017), though it adapted to the proposed control technique.

The paper is divided as follows: Section 2 introduces the boost converter model. Next, Section 3 presents the proposed control strategy. Section 4 shows the collected results and reports the controller performance. Finally, Section 5 discusses the main conclusions of the article.

2. BOOST CONVERTER MODEL

The proposed FMPC is applied to a DC-DC step-up converter. The model used is a 3SSC boost converter presented in Costa (2017). Figure 1 illustrates the topology of the converter. Besides, Table 1 provides the specifications of the circuit structure.

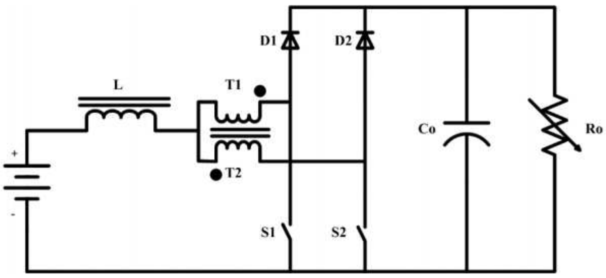

Figure 1. 3SSC Boost Converter (Costa, 2017).

Table 1. 3SSC boost converter electrical parameters.

Parameter	Values
Input Voltage (V_i)	26 – 36 [V]
Output Voltage (V_o)	48 [V]
Duty Cycle (D_{cycle})	0.25 – 0.46
Sample time (T_s)	1 [ms]
Inductor filter (L)	35 [μH]
Output capacitor (C_o)	4000 [μF]
Capacitor intrinsic resistance (R_{co})	26.7 [$m\Omega$]
Load resistance (R_o)	2.3 – 6.1 [$m\Omega$]
Output power (P_o)	380 – 1000 [W]

The continuous system model is represented by the medium state-space equations given in (1).

$$\begin{aligned} \dot{x} &= A_t x(t) + B_t u(t) \\ y(t) &= C_t x(t) + D_t u(t) \end{aligned} \tag{1}$$

where, the state variable is $x(t) = \left[\, i_L \; V_c \,\right]^t$, i_L is the inductor current and V_c the capacitor voltage. The output voltage is given by $y(t) = V_o(t)$ and $u(t)$ represents the control signal. The state-space matrices A_t, B_t, C_t and D_t are expressed in (2), (3), (4) and (5), respectively.

$$A_t = \begin{bmatrix} -\dfrac{R_L + (1-D_{cycle})(R_{co}||R_o)}{L} & -\dfrac{(1-D_{cycle})R_o}{L(R_{co}+R_o)} \\ \dfrac{(1-D_{cycle})R_o}{C_o(R_{co}+R_o)} & -\dfrac{1}{C_o(R_{co}+R_o)} \end{bmatrix} \tag{2}$$

$$B_t = \begin{bmatrix} \dfrac{R_{co}}{L}\dfrac{(1-D_{cycle})R_o + R_{co}}{(R_{co}+R_o)} \\ -\dfrac{R_o}{C_o(R_{co}+R_o)} \end{bmatrix} \left(\dfrac{V_i}{R'}\right) \tag{3}$$

$$C_t = \begin{bmatrix} (1-D_{cycle})(R_{co}||R_o) & \dfrac{R_o}{R_{co}+R_o} \end{bmatrix} \tag{4}$$

$$D_t = -V_i \frac{R_{co}||R_o}{R'}. \tag{5}$$

The term $R' = (1-D_{cycle})^2 R_o + D_{cycle}(1-D_{cycle})(R_{co}||R_o)$.

To evaluate the controller performance under disturbances, a variation in the operation point is applied to the converter. According to Costa (2017), the uncertainties of the 3SSC converter occur due to the change in the input voltage (V_i) and the output power (P_o). Thus, the 3SSC boost converter has two uncertain parameters, the load resistance (R_o), which changes depending on the output power (P_o), and the input voltage (V_i), which is a function of the duty cycle (D_{cycle}). These parameters are expressed in (6) and (7), respectively .

$$R_0 = f(P_o) = \frac{V_0^2}{P_o}, P_o \in [380, 1000]W \tag{6}$$

$$D_{cycle} = f(V_i) = 1 - \frac{V_i}{V_0}, V_i \in [26, 36]V \tag{7}$$

Joining (1), (6), and (7), the state space model can be represented as showed in (8).

$$\begin{aligned} \dot{x} &= A_t\left(P_o, V_i\right) x\left(t\right) + B_t\left(P_o, V_i\right) u\left(t\right) \\ y(t) &= C_t\left(P_o, V_i\right) x\left(t\right) + D_t\left(P_o, V_i\right) u\left(t\right) \end{aligned} \tag{8}$$

The model presented in (8) is a continuous Linear Time Variant (LTV) system. Discretizing (8) in the sample time displayed at Table 1, the system becomes (9).

$$\begin{aligned} x\left(k+1\right) &= A\left(P_o, V_i\right) x\left(k\right) + B\left(P_o, V_i\right) u\left(k\right) \\ y\left(k\right) &= C\left(P_o, V_i\right) x\left(k\right) + D\left(P_o, V_i\right) u\left(k\right) \end{aligned} \tag{9}$$

where the discretization method follows the one adopted by Costa (2017).

Using the polytopic structure in (9) and the variations in time showed in Figure 2, the vertices of the discretized system are given by (10)-(13).

$$\begin{aligned} &-f(36V, 1000W) \\ &A_1 = \begin{bmatrix} -0.2838 & -7.7479 \\ 0.0634 & -0.1136 \end{bmatrix} \quad B_1 = \begin{bmatrix} 580.4784 \\ 65.2796 \end{bmatrix}, \\ &C_1 = \begin{bmatrix} 0.0198 & 0.9885 \end{bmatrix} \qquad D_1 = -0.7304 \end{aligned} \tag{10}$$

$$\begin{aligned} &-f(26V, 1000W) \\ &A_2 = \begin{bmatrix} 0.0958 & -8.4508 \\ 0.0691 & 0,2660 \end{bmatrix} \quad B_2 = \begin{bmatrix} 851.9917 \\ 53.4467 \end{bmatrix}, \\ &C_2 = \begin{bmatrix} 0.0143 & 0.9885 \end{bmatrix} \qquad D_2 = -1.0054 \end{aligned} \tag{11}$$

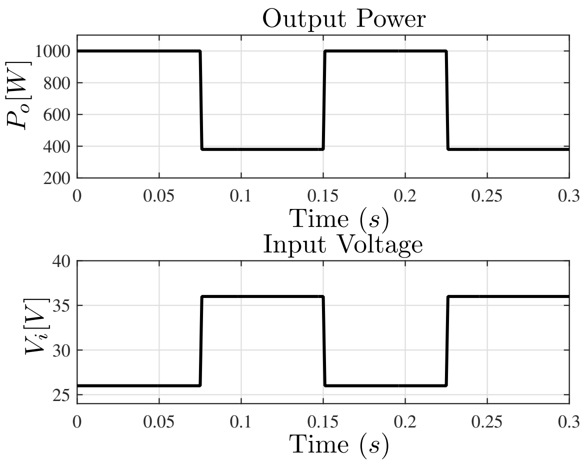

Figure 2. Variation in the operating point of the 3SSC converter.

$-f(36V, 380W)$

$$A_3 = \begin{bmatrix} -0.3102 & -7.9645 \\ 0.0652 & -0.1119 \end{bmatrix} \quad B_3 = \begin{bmatrix} 542.7337 \\ 68.8140 \end{bmatrix} \tag{12}$$
$$C_3 = [\,0.01993\ 0.9956\,] \qquad D_3 = -0.2802$$

$-f(26V, 380W)$

$$A_4 = \begin{bmatrix} 0.0759 & -8.7329 \\ 0.0715 & 0.2873 \end{bmatrix} \quad B_4 = \begin{bmatrix} 814.2744 \\ 58.5879 \end{bmatrix} \tag{13}$$
$$C_4 = [\,0.0144\ 0.9956\,] \qquad D_4 = -0.3871$$

3. CONTROL STRATEGY

The proposed control strategy combines the MPC with Fuzzy Control, the theoretical aspects of these techniques are introduced in this section. Subsection 3.1 formulates the augmented state space model applied to the 3SSC Converter. Subsequently, subsection 3.2 discusses the T-S fuzzy model for the system. Furthermore, subsection 3.3 introduces the FMPC control law and subsection 3.4 defines the implemented offline algorithm. Lastly, the block diagram for the control system is illustrated in subsection 3.5.

3.1 Augmented state space model

Following what was presented in Costa (2017), a integral control with two degree-of-freedom is added to the proposed scheme. Such control is adjusted by the variables g and h, which are adopted as $g = 1$ and $h = 10$ in order to guarantee the best performance.

The augmented model for the 3SSC Boost Converter is represented by (14).

$$\begin{aligned} x(k+1) &= \hat{A}_j x(k) + \hat{B}_j u(k) \\ y(k) &= \underbrace{[C_j \quad 0]}_{\hat{C}_j} + \underbrace{\begin{bmatrix} D_j \\ 0 \end{bmatrix}}_{\hat{D}_j} \end{aligned} \tag{14}$$

With,

$$\hat{A}_j = \begin{bmatrix} A_j & 0 \\ -hC_j & g \end{bmatrix} \quad \hat{B}_j = \begin{bmatrix} B \\ -hD_j \end{bmatrix} \tag{15}$$

$j = 1, \ldots, N$, com N representando a quantidade de vértices do sistema.

3.2 Takagi-Sugeno Fuzzy model

The augmented model presented in (14) is used to implement the FMPC proposed by Yeh et al. (2006). In order to perform this technique the converter model must be represented using the T-S fuzzy inference system. Wang (1997) defines a T-S fuzzy model as a representation of a nonlinear system through locals linear input-output relationship.

Thus, a discrete T-S fuzzy system is characterized through IF-THEN rules for its i-th subsystems, as shown in (16),

$$Rule\ i: \begin{cases} If \quad Z_1(k) = \mu_{i1} ... \ and \ \ Z_p(k) = \mu_{ip} \\ Then \quad x(k+1) = \hat{A}_i x(k) + \hat{B}_i u(k) \end{cases} \tag{16}$$

where $Z_1(k)$, $Z_2(k), \ldots,$ $Z_p(k)$ are the premise variables, μ_{ij} are the memberships degrees, $\hat{A}_i \in R^{nxn}$ and $\hat{B}_i \in R^{nxm}$ are the augmented state matrices, with $i = 1, 2, \ldots, r$, being r the number of rules.

The global output is expressed by (17).

$$x(k+1) = \sum_{i=1}^{r} h_i(Z(k)(\hat{A}_i x(k) + \hat{B}_i u(k))) \tag{17}$$

Where $h_i(Z(k))$ represents the weight of each rule and is given by (18).

$$h_i(Z(k)) = \frac{w_i(Z(k))}{\sum_{i=1}^{r} w_i(Z(k))} \tag{18}$$

With,

$$w_i(Z(k)) = \prod_{l=1}^{p} M_{il}(Z(k)) \tag{19}$$

Moreover, the PDC is used to obtain the control law, as given in (20).

$$u(k) = \left(\sum_{i=1}^{r} h_i(Z(k)) F_i \right) x(k) \tag{20}$$

Where, F_i represents the gain associated with each fuzzy rules.

To represent the 3SSC boost converter through fuzzy logic a two-rules T-S fuzzy system is implemented. Using the the duty cycle as input variable, which is a function of the input voltage, as expressed by (7). The fuzzy layout of this variable is done through trapezoidal membership functions, illustrated in Figure 3.

3.3 Fuzzy Model Predictive Control

Following Yeh et al. (2006), the FMPC control law is implemented using the Linear Matrix Inequalities (LMI) approach. This method allows to deal with uncertainties and add constraints to the system.

This strategy consists of calculating, at each sample time, a state-feedback control law that minimizes the cost function given in (21).

$$\underset{u(k)}{min} \ \ \underset{\Omega}{max} \ \ J_\infty(k), \tag{21}$$

where

$$J_\infty(k) = \sum_{i=0}^{\infty} [\hat{X}(k+i) + U(k+i)], \tag{22}$$

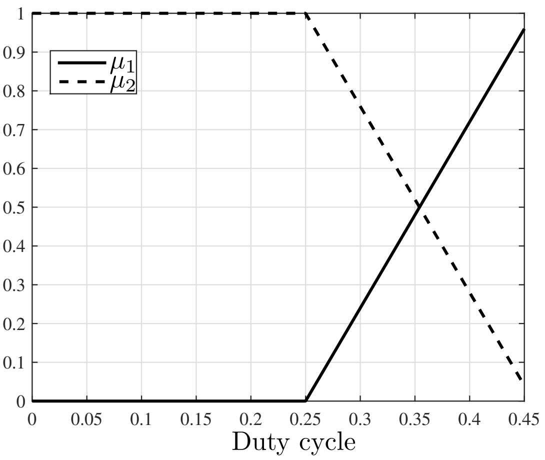

Figure 3. Membership Functions.

with

$$\begin{aligned} \hat{X}(k+i) &= \hat{x}(k+i|k)^T W \hat{x}(k+i|k), \\ U(k+i) &= u(k+i|k)^T R u(k+i|k), \end{aligned} \tag{23}$$

$\hat{x}(k) \in R^{n_x}$ is the augmented state vector, $u(k) \in R^{n_u}$ is the input signal and $y(k) \in R^{n_y}$ represents the output signal. $W = W^T \geq 0$ and $R = R^T > 0$ are symmetric weighting matrices and Ω is the convex hull of plant model $[\hat{A}(k+i)\ \hat{B}(k+i)] \in \Omega,\ i \geq 0$.

Therefore, FMPC can be described as the LMI problem in (24), considering the augmented system with its model uncertain designed by polytopes.

$$\min_{\gamma,\ Q,\ Y_i} \quad \gamma \tag{24}$$

subject to the constraints given in (25)-(27).

$$\begin{bmatrix} 1 & x(k|k) \\ x(k|k)^T & Q \end{bmatrix} \geq 0 \tag{25}$$

$$\begin{bmatrix} Q & * & * & * \\ \hat{A}_j Q + \hat{B}_j Y_j & Q & * & * \\ W^{\frac{1}{2}} Q & 0 & \gamma I & * \\ R^{\frac{1}{2}} Y_j & 0 & 0 & \gamma I \end{bmatrix} \geq 0 \tag{26}$$

$$\begin{bmatrix} 4Q & * & * & * & * \\ S & Q & * & * & * \\ \sqrt{2} W^{\frac{1}{2}} Q & 0 & \gamma I & * & * \\ \sqrt{2} R^{\frac{1}{2}} Y_j & 0 & 0 & \gamma I & * \\ \sqrt{2} R^{\frac{1}{2}} Y_i & 0 & 0 & 0 & \gamma I \end{bmatrix} \geq 0 \tag{27}$$

Where, $S = A_j Q + B_j Y_i + A_i Q + B_i Y_j$.

Moreover, the constraints $\|u(k)\|_2 \leq u_{max}$ and $\|y(k)\|_2 \leq y_{max}$ are assured if the constraints given in (28) and (29), respectively, are followed.

$$\begin{bmatrix} Q & * \\ Y_j & u_{max}^2 I \end{bmatrix} \geq 0 \tag{28}$$

$$\begin{bmatrix} Q & * \\ C_j \dfrac{S}{2} & y_{max}^2 I \end{bmatrix} \geq 0 \tag{29}$$

The feedback gains for the FMPC can be obtained by (30).

$$F_i = Y_i Q^{-1} \tag{30}$$

3.4 Offline algorithm

Considering the FMPC control law given in subection 3.3 and the converter fuzzy model in subsection 3.2, the proposed offline FMPC algorithm method is obtained as follows:

For an offline system, given an initial condition x_2, a sequence of minimizers (γ, Q, Y_i, Y_j) is calculated following (21)-(29). *Take k:=1*

- *Compute the minimizers (γ, Q, Y_i, Y_j) with the additional constraints $Q > 0$ and $Q = Q^T$ and keep Q, Y_i and F_i in a lookup table;*
- *If $i < N$, choose the state $(x_2)_{k+1}$ satisfying $\|x_{k+1}\|_{Q^{-1}} \leq 1$. Take k:=k+1 and go to step one.*

Lookup table: given the initial condition $\|x(0)\|_{Q^{-1}} \leq 1$ take the state $x(k)$ for the respective time k. Plot the search around Q^{-1} in the lookup table to find the biggest j (or the smallest ellipsoid).

Apply the control law (20).

3.5 Block Diagram

Based on the exposed in the aforementioned subsections, Figure 4 displays the block diagram for the proposed augmented FMPC applied to the 3SSC boost converter.

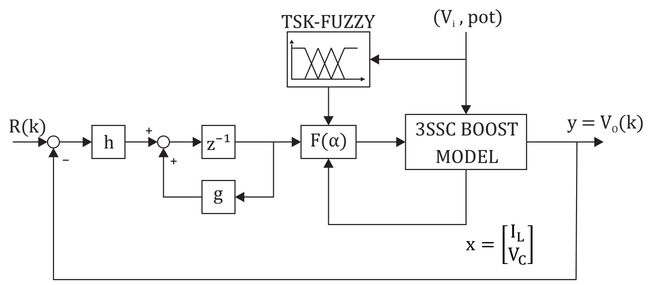

Figure 4. Block diagram.

4. RESULTS ANALYSIS

This section discusses the obtained results for the FMPC applied to the discretized 3SSC boost converter. The controller performance is analyzed through time response, stability ellipsoids, and performance metrics. Furthermore, a comparison between FMPC and LQI control is presented.

Figure 5 shows the output response for the FMPC in comparison with the classic LQI control law. It can be seen that both controllers are able to follow the reference tracking even after changing the operation point, presenting oscillations only at these moments. However, the FMPC has a faster and stabler performance, presenting less oscillations and lower overshoots and undershoots.

The control signals are illustrated in Figure 6, showing once again a better performance of the proposed controller. Since the LQI control law presented a slower and more oscillatory outcome. Moreover, the input constraint $|u(k)| < 1,\ k \geq 0)$ is satisfied.

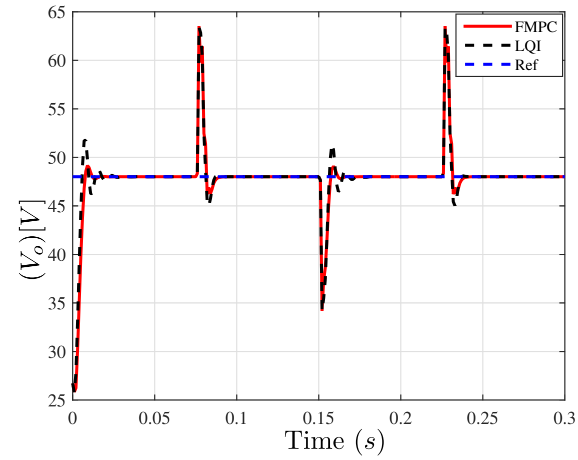

Figure 5. Output response $y(k)$=$V_o(k)$.

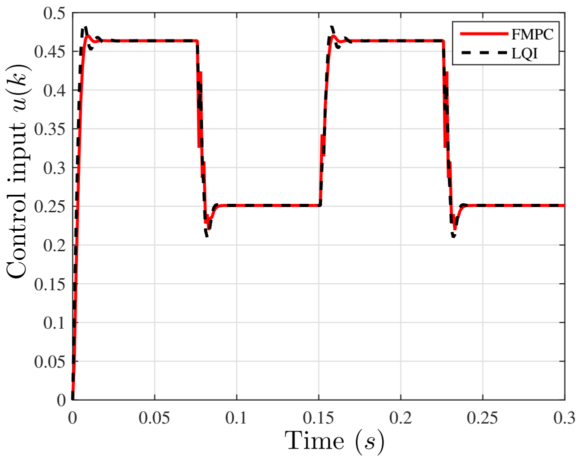

Figure 6. Control signal $u(k)$.

The stability performance of the controller is assessed using invariant ellipsoids. Following Costa (2017), for the 3SSC boost converter, the worst condition is the impulse response. Thus, if the system's impulse response remains within the ellipsoid boundaries and this response tends to zero on steady state, then the system is stable.

The first step in this kind of analysis is to obtained the impulse response considering the nominal operating point. Thus, considering that the converter nominal condition is given in (10), a set of twenty voltage points was obtained to design the ellipsoid, given by $x_{2_{set}} = [48.0000\ -3.6942\ -23.6553\ 11.3360\ 7.8756\ -9.0638\ -0.5195\ 4.9506\ -1.6958\ -1.9171\ 1.6496\ 0.3478\ -1.0017\ 0.2161\ 0.4384\ -0.2874\ -0.1152\ 0.1962\ -0.0177\ -0.0957\ 0.0473]$.

Figure 7 presents the ellipsoids for the matrices Q_i, with $i = 1,\ 2, ..., 20$, considering the set $x_{2_{set}}$. Analyzing Figure 7, the the closed-loop stability can be verified, since the size of the ellipsoids decreases as i approaches 20.

Furthermore, Figure 8 displays the projection for the impulse response for each N ellipsoid. According to Costa (2017), the closed loop system is stable to any value of N; Thus, choosing the ellipsoid N=20 the trajectory of the impulse response for the controller is illustrated in Figure 9. It is possible to notice that the impulse response is

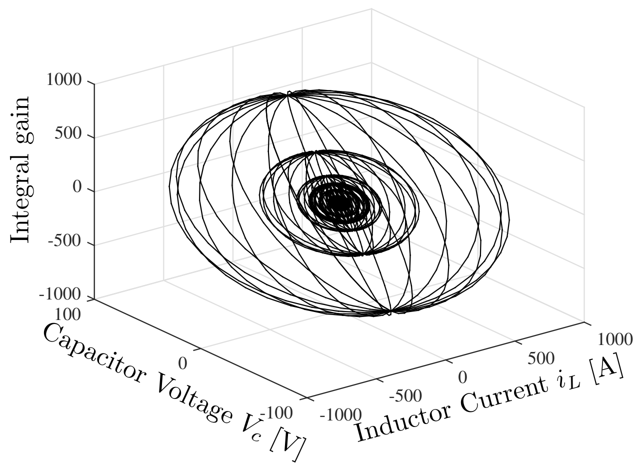

Figure 7. Stability Ellipsoids.

restricted inside the limits of the ellipsoid. In addition, the impulse response converge to the origin, thus it can be concluded that the proposed controller guarantees the system stability.

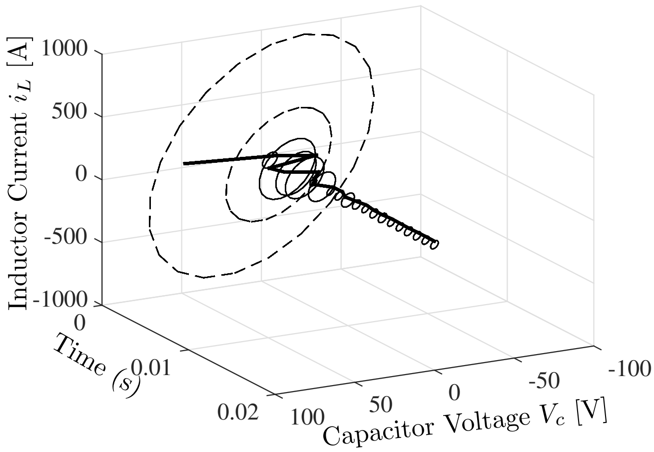

Figure 8. The closed-loop impulse response bounded by ellipsoids in $x_{set} \times i_L \times V_c$.

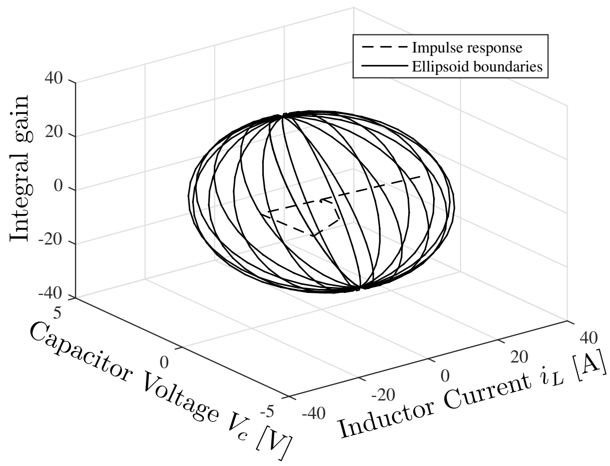

Figure 9. Impulse response for N=20.

The controller was also evaluated and compared using the cost function given in (14) as a performance index. The result obtained for the FMPC is $J_\infty = 9.9627 \times 10^5$ while for the LQI $J_\infty = 1.0062 \times 10^6$, reinforcing the superiority of the FMPC in comparison with LQI.

5. CONCLUSION

The designed procedure demonstrate the effectiveness of the FMPC, taking into consideration the time response with variations of the input voltage and the load, and also the J_∞ performance index. In addition, the FMPC exhibited satisfactory results considering the ellipsoid stability analysis for the offline representation. Therefore, compared to the LQI under the same design conditions, the offline FMPC controller proved its viability application for 3SSC boost converters.

ACKNOWLEDGEMENTS

This study was financed in part by the Coordenação de Aperfeiçoamento de Pessoal de Nível Superior - Brasil (CAPES) - Finance Code 001. The authors would like to thank the Federal Rural University of the Semi-Arid Region (UFERSA) and the Research Group on Automation and Control (GEAC) (financial provided by PIG00009-2018 project) for their support and support in the production of this work.

REFERENCES

Abbasi, S.M.M. and Jalali, A. (2020). Fuzzy tracking control of fuzzy linear dynamical systems. *ISA transactions*, 97, 102–115.

Bartsch, A.G., Teixeira, J.R., de Oliveira, J., and Cavalca, M.S. (2019). Procedures to design multi-model-based predictive controller applied to bldc drive. *Journal of Control, Automation and Electrical Systems*, 30(6), 994–1006.

Camacho, E.F. and Bordons, C. (2007). *Model Predictive Control*. Springer, London.

Capron, B.D.O. and Odloak, D. (2013). Lmi-based multi-model predictive control of an industrial c3/c4 splitter. *Journal of Control, Automation and Electrical Systems*, 24(4), 420–429.

Costa, M.V.S. (2017). *Controle MPC robusto aplicado ao conversor boost ccte otimizado por inequações matriciasi lineares*. Ph.D. thesis, Universidade Federal do Ceará, Fortaleza.

Espinosa, J.J., Hadjili, M.L., Wertz, V., and Vandewalle, J. (1999). Predictive control using fuzzy models—comparative study. In *1999 European Control Conference (ECC)*, 1511–1516. IEEE.

Fateh, S. and Fateh, M.M. (2020). Adaptive fuzzy control of robot manipulators with asymptotic tracking performance. *Journal of Control, Automation and Electrical Systems*, 31(1), 52–61.

Khairy, M., Elshafei, A.L., and Emara, H.M. (2010). Lmi based design of constrained fuzzy predictive control. *Fuzzy Sets and Systems*, 161(6), 893–918.

Kothare, M.V., Balakrishnan, V., and Morari, M. (1996). Robust constrained cmamodel predictive control using linear matrix inequalities. *Automatica*, 32(10), 1361–1379.

Kovacic, Z. and Bogdan, S. (2006). *Fuzzy controller design: theory and applications*. CRC press, Fort Worth.

Lu, Y. (2018). Adaptive-fuzzy control compensation design for direct adaptive fuzzy control. *IEEE Transactions on Fuzzy Systems*, 26(6), 3222–3231.

Luong, D. and Tsao, T.C. (2014). Linear quadratic integral control of an organic rankine cycle for waste heat recovery in heavy-duty diesel powertrain. In *2014 American control conference*, 3147–3152. IEEE.

Maccari Jr, L., Lima, D., Koch, G., and Montagner, V. (2019). Robust model predictive controller applied to three-phase grid-connected lcl filters. *Journal of Control, Automation and Electrical Systems*, 1–14.

Méndez, J.A., Marrero, A., Reboso, J.A., and León, A. (2016). Adaptive fuzzy predictive controller for anesthesia delivery. *Control Engineering Practice*, 46, 1–9.

Rego, R.C.B. and Costa, M.V.S. (2020). Output feedback robust control with anti-windup applied to the 3ssc boost converter. *IEEE Latin America Transactions*, 18(05), 874–880.

Sari, N.N., Jahanshahi, H., and Fakoor, M. (2019). Adaptive fuzzy pid control strategy for spacecraft attitude control. *International Journal of Fuzzy Systems*, 21(3), 769–781.

Takagi, T. and Sugeno, M. (1985). Fuzzy identification of systems and its applications to modeling and control. In *IEEE Trans. Syst. Man. Cyber*, volume 15, 116–132. Elsevier.

Teng, L., Wang, Y., Cai, W., and Li, H. (2017). Robust model predictive control of discrete nonlinear systems with time delays and disturbances via t–s fuzzy approach. *Journal of Process Control*, 53, 70–79.

Treesatayapun, C. (2019). Fuzzy rules emulated discrete-time controller based on plant's input–output association. *Journal of Control, Automation and Electrical Systems*, 30(6), 902–910.

Vazquez, S., Rodriguez, J., Rivera, M., Franquelo, L.G., and Norambuena, M. (2016). Model predictive control for power converters and drives: Advances and trends. *IEEE Transactions on Industrial Electronics*, 64(2), 935–947.

Wang, L.X. (1997). *A course in fuzzy systems and control*, volume 2. Prentice Hall PTR Upper Saddle River, NJ.

Wang, L. (2009). *Model predictive control system design and implementation using MATLAB®*. Springer Science & Business Media.

Wang, X., Li, S., Su, S., and Tang, T. (2018). Robust fuzzy predictive control for automatic train regulation in high-frequency metro lines. *IEEE Transactions on Fuzzy Systems*, 27(6), 1295–1308.

Wu, X., Shen, J., Li, Y., and Lee, K.Y. (2015). Fuzzy modeling and predictive control of superheater steam temperature for power plant. *ISA transactions*, 56, 241–251.

Yeh, S., Ji, D., Yoo, W., and Won, S. (2006). Efficient fuzzy-mpc for nonlinear systems: rule rejection. In *2006 SICE-ICASE International Joint Conference*, 5653–5657. IEEE.

Yu-Geng, X., De-Wei, L., and Shu, L. (2013). Model predictive control—status and challenges. *Acta Automatica Sinica*, 39(3), 222–236.